



HAL
open science

Molecular Diversity and Amino Acid Evolution in Simulated Carbonaceous Chondrite Parent Bodies

Adeline Garcia, Yingfei Yan, Cornelia Meinert, Philippe Schmitt-Kopplin, Vassilissa Vinogradoff, Jean-Christophe Viennet, Laurent Remusat, Sylvain Bernard, Michel Righezza, Louis Le Sergeant D'hendecourt, et al.

► **To cite this version:**

Adeline Garcia, Yingfei Yan, Cornelia Meinert, Philippe Schmitt-Kopplin, Vassilissa Vinogradoff, et al.. Molecular Diversity and Amino Acid Evolution in Simulated Carbonaceous Chondrite Parent Bodies. ACS Earth and Space Chemistry, 2024, 8 (3), pp.606-615. 10.1021/acsearthspacechem.3c00366 . hal-04731789

HAL Id: hal-04731789

<https://hal.science/hal-04731789v1>

Submitted on 11 Oct 2024

HAL is a multi-disciplinary open access archive for the deposit and dissemination of scientific research documents, whether they are published or not. The documents may come from teaching and research institutions in France or abroad, or from public or private research centers.

L'archive ouverte pluridisciplinaire **HAL**, est destinée au dépôt et à la diffusion de documents scientifiques de niveau recherche, publiés ou non, émanant des établissements d'enseignement et de recherche français ou étrangers, des laboratoires publics ou privés.

1 **Molecular diversity and amino acids evolution in simulated carbonaceous chondrites parent bodies.**

2 A. Garcia¹, Y. Yan^{2,3}, C. Meinert⁴, P. Schmitt-Kopplin^{2,3}, V. Vinogradoff¹, J-C Viennet^{5,6}, L. Remusat⁵, S.
3 Bernard⁵, M. Righetta¹, L. Le Sergeant d'Hendecourt¹, G. Danger^{1,7*}

4 ¹ Aix-Marseille Université, CNRS, Institut Origines, Laboratoire PIIM, Marseille, France

5 ² Helmholtz Zentrum München, Analytical BioGeoChemistry, Neuherberg, Germany.

6 ³ Technische Universität München, Chair of Analytical Food Chemistry, Freising-Weihenstephan, Germany.

7 ⁴ Université Côte d'Azur, Institut de Chimie de Nice, UMR 7272 CNRS, F-06108 Nice, France

8 ⁵ Muséum National d'Histoire Naturelle, Sorbonne Université, UMR CNRS 7590, Institut de minéralogie, de
9 physique des matériaux et de cosmochimie, Paris, France

10 ⁶ Université de Lille, CNRS, INRAE, Centrale Lille, UMR 8207-UMET-Unité Matériaux et Transformations, F-
11 59000 Lille, France

12 ⁷ Institut Universitaire de France (IUF), France

13 *gregoire.danger@univ-amu.fr

14 **ABSTRACT:**

15 Organic matter in interplanetary bodies, particularly in parent bodies of carbonaceous chondrites, displays
16 diverse molecules generated in different environments of the Solar nebula. In this study, we simulate the solid
17 phase environment in the laboratory to trace the step-by-step evolution of organic matter from dense molecular
18 cloud ices to processes in meteorite parent bodies. This evolution have shown to lead to an important molecular
19 diversity. Among molecules formed, we focus on amino acids considered as possible chemical tracers of
20 secondary alteration on asteroids. Using gas chromatography and high-resolution mass spectrometry, we
21 detected amino acids in trace amounts in a pre-accretional organic analog formed from dense molecular ice
22 analogs. This analog was then subjected to aqueous alteration at different temperatures and durations. Water
23 induced a complex reactivity leading to increased formation of α - and β -amino acids over time. The initial
24 formation involved reactions between sugars and amine compounds, followed by amino acid destruction, due to
25 the Maillard reaction consuming both sugars and amino acids, hypothesis supported by high resolution mass
26 spectrometry data. Surprisingly, a second phase of amino acid formation, specifically α -amino acids, was
27 observed, indicating the possible occurrence of the Strecker reaction. These findings demonstrate the complex
28 chemical network occurring in presence of a molecular diversity as possibly taking place during parent body
29 alteration. This implies that amino acids detected in various meteorites could have formed through different
30 pathways depending on the initial content of amino acid precursors and on the level and duration of the aqueous
31 alteration.

32

33 Keywords: amino acids, GC-FT-Orbitrap-MS, gas chromatography, high-resolution mass spectrometry, ice
34 analogs, meteorite.

35

36 **1. INTRODUCTION**

37 Studying comets and asteroids can provide insight into the origins of our solar system ¹. These objects are
38 believed to have undergone minimal alterations since their formation ², making them valuable probes of the early
39 history of the solar system. Space probes such as Rosetta have analyzed the organic content of comets like
40 67P/Tchourioumov-Guerassimenko and found a high molecular diversity, including both organic and inorganic
41 compounds ³. The Hayabusa2 mission also discovered a significant molecular diversity on the surface of the
42 Ryugu asteroid ⁴, with amino acids ⁵ and nucleobases ⁶ being identified through targeted analyses. Additionally,
43 carbonaceous chondrites provide information on the organic content of asteroids⁷, with up to 5% of their weight
44 being organic matter divided into insoluble and soluble fractions. Both fractions present an important molecular
45 diversity ^{8,9}. The insoluble fraction may consist of hydrophobic macromolecules interacting with smaller
46 hydrophobic molecules ⁹, while the soluble fraction presents the highest molecular diversity, containing

47 polyaromatic hydrocarbons, sugars, nucleobases as well as amino acids ¹⁰⁻¹³. Some of these amino acids have
 48 been detected with slight enantiomeric excesses, which could provide a possible scenario for the emergence of
 49 homochirality on Earth. These meteoritic amino acids may also serve as markers of chemical evolution of parent
 50 bodies ^{14,15} as different chemical reactions can lead to their formation depending on their configuration,
 51 precursors, and/or environment.

52 However, meteorites only reveal the final stage of evolution of their parent body history. Laboratory experiments
 53 have been developed to obtain a comprehensive understanding of the origin and evolution of organic matter in
 54 asteroids and comets. These experiments simulate the evolution of dense molecular cloud ices that occurred
 55 during the formation and evolution of the solar nebula. Small molecules like H₂O, NH₃, CH₃OH, CO₂, and CO
 56 are deposited onto a cold substrate to form an analog of interstellar ices observed in dense molecular clouds.
 57 When these ice analogs are exposed to energetic particles, such as UV photons at Lyman α , ion or electrons
 58 bombardment, and subsequently warmed to 300 K to simulate the natural evolution of minor bodies in the solar
 59 system, a significant molecular diversity is generated ¹⁶. Targeted analyses of these experiments have detected
 60 nucleobases ^{17,18}, sugars ¹⁹ and amino acids ²⁰; suggesting that the protoplanetary disk were already rich in
 61 organic molecules before accretion. Comparisons between the amino acid content of such pre-accretional
 62 laboratory analog and CM meteorites recovered after the same treatment with acid hydrolysis at 100 °C, a
 63 procedure generally used to recover amino acids in meteorites, reveal similarities between that pre-accretional
 64 laboratory analogs and the least altered CM chondrites ²¹. However, pre-accretional analogs still differ from the
 65 organic content of meteorites ²² likely due to the secondary evolution happening in the meteorite parent bodies
 66 that influences the molecular inventory.

67 To simulate this evolution, pre-accretional ice analogs were subjected to aqueous alteration in laboratory
 68 experiments. This resulted in the complete transformation of its molecular content ²³ while retaining molecular
 69 diversity. In this contribution, new experiments are presented on the simulation of the formation and evolution of
 70 organic matter from molecular ices in dense clouds to its incorporation inside asteroids, where it may have
 71 undergone an aqueous reaction. In this study, the evolution of amino acids was monitored depending on
 72 temperature and duration of experiments to obtain information on chemical pathways leading to amino acids in
 73 the presence of a high molecular diversity. Analyses were performed using a gas chromatography coupled to
 74 high-resolution mass spectrometer (GC-FT-Orbitrap-MS). The amino acids were initially searched for in the pre-
 75 accretional analog, and after its incubation at different temperatures (5 °C and 150 °C) for up to 100 days.
 76 Different evolution patterns were observed based on the amino acid configurations (α vs. β), suggesting distinct
 77 chemical pathways occurring at various times. FT-ICR data from our previous work ²³ were also used to
 78 strengthen hypotheses of proposed reaction.

79 2. RESULTS

80 A pre-accretional analog was formed from a photo-processed ice mixture of H₂O:CH₃OH:NH₃ with a ratio of
 81 3:1:1 at Lyman α and 77 K. The experimental procedure leads to the formation of an important molecular
 82 diversity as demonstrated by previous work ^{16,24}. GC-FT-orbitrap-MS was used to identify amino acids following
 83 their derivatization ²⁵. To avoid any analytical bias due to potential contamination of biological L-amino acids,
 84 only the D form of chiral amino acids was reported here, utilizing enantioselective separation.

85

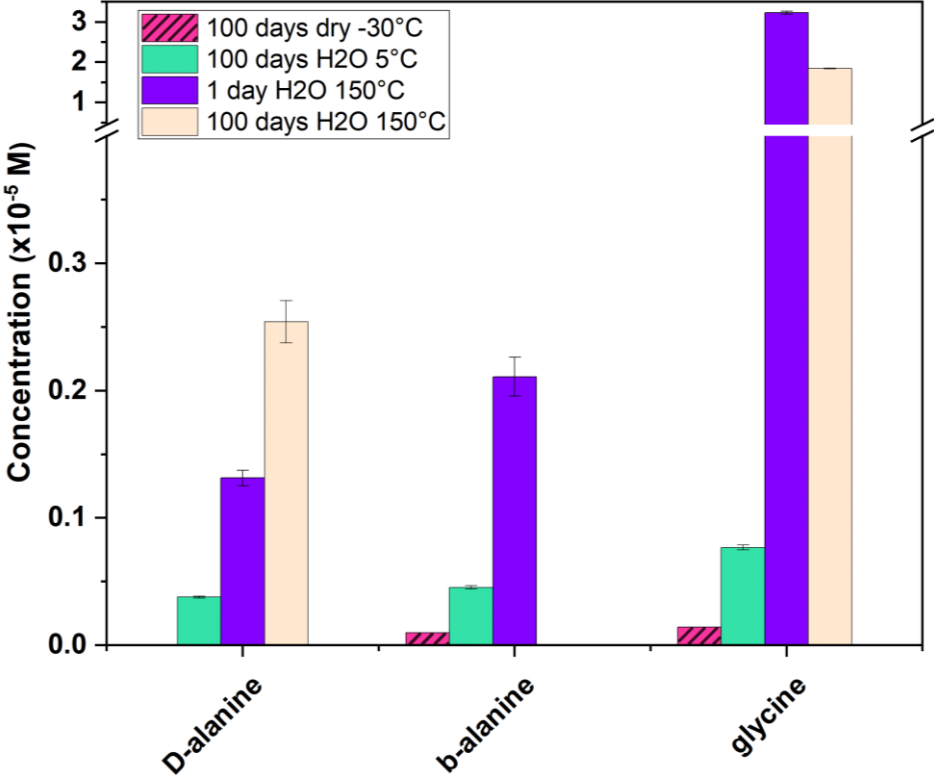
86 **Table 1 – Amino acids identified in the pre-accretional analog before (stored at -30 °C) and after different**
 87 **chemical treatments, (with 6N HCl at 110 °C, in pure H₂O at 5°C or 150°C for 1 or 150 days). id:**
 88 identified/non-quantified, nd: non-detected.

Amino acids	configuration		stored dry at -30°C *	Pre-accretional analog							
				6N HCl 110 °C		H ₂ O 5 °C		H ₂ O 150 °C			
	#C	α or β		1 day concentration (M)	σ (%)	100 days concentration (M)	σ (%)	1 day concentration (M)	σ (%)	100 days concentration (M)	σ (%)
glycine	2	α	id	5.36×10^{-4}	3.7	7.70×10^{-7}	2.6	3.23×10^{-5}	1.2	1.85×10^{-5}	0.5%
D-alanine	3	α	nd	9.27×10^{-5}	2.3	3.80×10^{-7}	2.0	1.34×10^{-6}	4.6	2.54×10^{-6}	6.5%
β -	3	β	id	1.08×10^{-5}	4.6	id		2.11×10^{-6}	7.2	nd	

alanine											
sarcosine	3	α	id	2.09×10^{-5}	2.3	1.01×10^{-7}	3.7	1.58×10^{-6}	4.5	1.69×10^{-6}	2.8
D-2-ABA	4	α	nd	2.41×10^{-6}	1.7	nd		id		2.01×10^{-7}	5.0
D-3-ABA	4	β	nd	id		nd		id		nd	
D-aspartic acid	4	α	id	id		id		id		nd	
D-valine	5	α	nd	id		nd		nd		id	
D-leucine	6	α	nd	id		id		nd		id	

89 * The pre-accretional analog was stored at $-30\text{ }^{\circ}\text{C}$ under dry condition to limit its potential evolution.

90 Initially, the presence of only four amino acids (glycine, β -alanine, sarcosine and D-aspartic acid) was detected in
 91 the untreated pre-accretional analog (stored in dry conditions at $-30\text{ }^{\circ}\text{C}$). A fraction of this analog sample was
 92 incubated in water at $5\text{ }^{\circ}\text{C}$, resulting in an increase of detected amino acids after 100 days. D-alanine and D-
 93 leucine were additionally detected to the initial four amino acids, while the concentration of glycine and β -
 94 alanine also increased significantly (estimated at six times for glycine) (Figure 1). This observation indicates that
 95 the pre-accretional analog is highly reactive even at low temperature and contains amino acid precursors. After
 96 just one day of reaction simulating aqueous alteration at $150\text{ }^{\circ}\text{C}$, seven amino acids were detected, including
 97 glycine, D-alanine, β -alanine, sarcosine, D-2-ABA, D-3-ABA, and D-aspartic acid, but larger α -amino acids, D-
 98 valine and D-leucine, were not observed. The concentrations of D-alanine and β -alanine were multiplied by ten,
 99 and that of glycine by 100 compared to 100 days at $5\text{ }^{\circ}\text{C}$ (Figure 1). After 100 days at $150\text{ }^{\circ}\text{C}$, D-valine and D-
 100 leucine were observed, but β -amino acids and D-aspartic acid were no longer detected (Table 1). A fraction of
 101 the initial pre-accretional analog was also treated with 6N HCl at $110\text{ }^{\circ}\text{C}$ for 24h, which is commonly performed
 102 to investigate amino acids in water extracts of meteorites. This treatment led to a significant increase in the
 103 number and concentration of detected amino acids compared to the untreated sample (Figure S1). All previously
 104 identified amino acids were present, including glycine, D-alanine, β -alanine, sarcosine, D-2-ABA, D-3-ABA, D-
 105 aspartic acid, D-valine and D-leucine. Moreover, their concentration increased significantly compared to the non-
 106 treated sample (Figure S1). This proves that the pre-accretional analog, as well as water extracts of meteorite,
 107 contain amino acid precursors that can easily undergo hydrolysis.



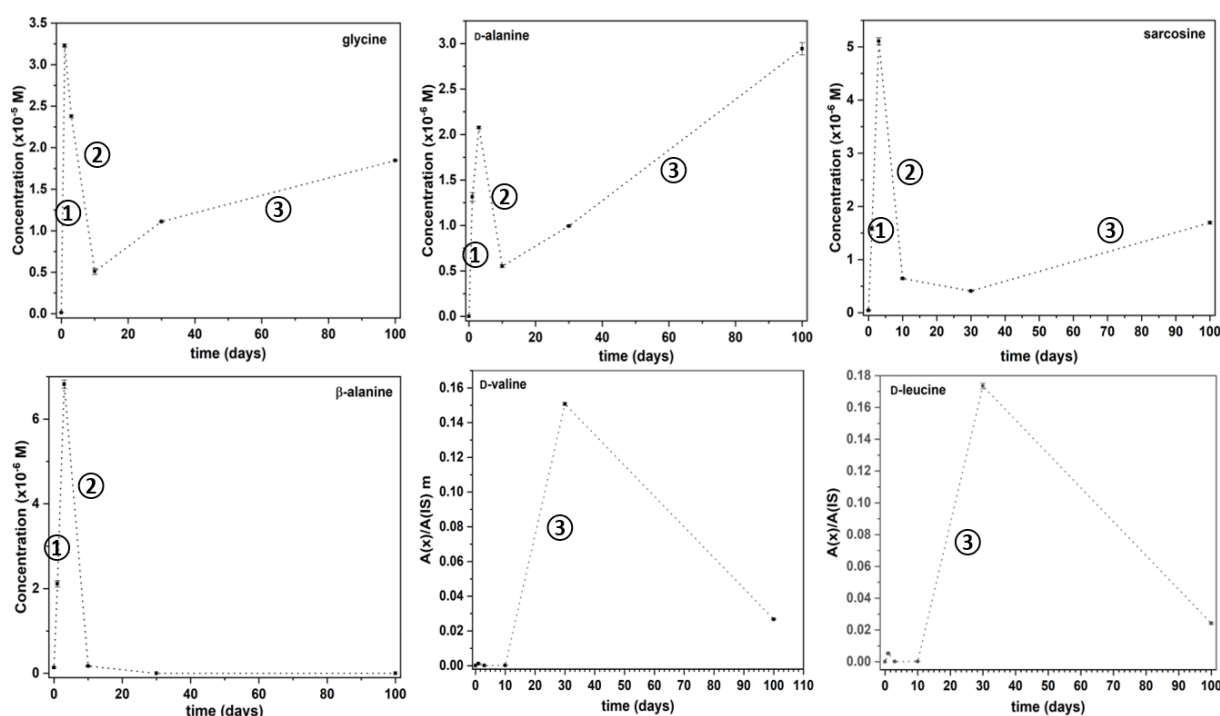
108

109 **Figure 1 – Concentration of D-alanine, β -alanine and glycine for the initial pre-accretional analog (stored**
 110 **at $-30\text{ }^{\circ}\text{C}$ under dry condition), and after 100 days in water at $5\text{ }^{\circ}\text{C}$ or $150\text{ }^{\circ}\text{C}$. β -Alanine and glycine in the**

111 pre-accretional analog (dry at -30 °C) are dashed because their detected peak areas are below the
112 quantification limit.

113 The evolution of the time profile of the amino acids presented in Table 1 was monitored at a temperature of
114 150 °C. The only amino acids that could be quantified were glycine, D-alanine, sarcosine and β -alanine. For the
115 remaining amino acids, only a qualitative profile based on absolute intensities is discussed. Figure 2 and S2
116 depict the overall evolution of amino acids (in concentration or absolute intensities), revealing three distinct
117 evolution profiles. A rapid increase in amino acid abundances occurs during the first 3 days of incubation, with
118 the exception of D-valine and D-leucine, which were not identified. After one day for glycine and 3 days for
119 other amino acids, there was a significant decrease in their abundance. Notably, after 10 days of incubation, the
120 evolution of amino acids varied depending on their configuration. The β -amino acids, such as β -alanine and D-3-
121 ABA, tend to disappear completely, while α -amino acids present a new increase in their abundances, including
122 the notable emergence of D-valine and D-leucine. Only α -aspartic acid showed a similar profile to β -amino acids.
123 After 30 days of incubation, D-valine and D-leucine tend to decrease, while other α -amino acids continue to
124 increase. These distinct evolution patterns suggest the occurrence of various chemical pathways.

125



126

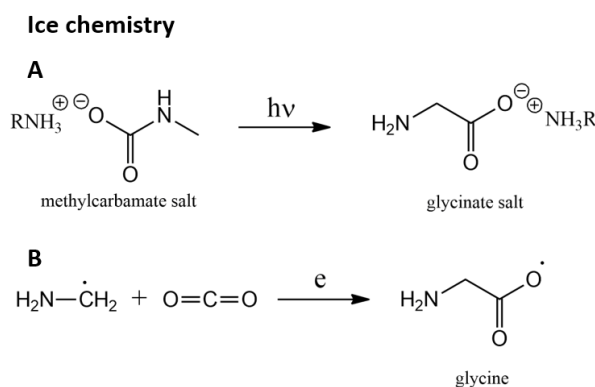
127 **Figure 2 –Monitoring of several amino acids in a pre-accretional analog incubated in water at 150 °C. The**
128 **different phases of amino acid evolution are also indicated as ①, ② and ③. More details on these different**
129 **phases are discussed in the main text. For glycine, alanine, sarcosine and β -alanine, quantifications are**
130 **performed by following the procedure published in Garcia *et al.* 2023. For valine and leucine with**
131 **abundances lower than their LOQ, only the qualitative evolution $A_{(x)}/A_{(IS)}$ of their relative integrated area**
132 **($A_{(x)}$) to the one of internal standard ($A_{(IS)}$) are displayed. The dotted lines are reported solely as a visual**
133 **guide.**

134 3. DISCUSSION

135 The organic material of the pre-accretional analog is highly reactive and efficiently evolves in the presence of
136 water, as demonstrated by the experiment in H₂O conducted at 5 °C and 150°C. There is a significant chemical
137 evolution at the molecular level. The high molecular diversity of the analog¹⁶ results in various chemical
138 reactions, affecting amino acid formation.

139 The initial analog (stored under dry condition at -30 °C) exhibits a low diversity and abundance of amino acids.
140 Glycine, β -alanine, sarcosine and aspartic acid are only detected as trace amounts below their limit of
141 quantification. These amino acids are directly related to the photo-processing of the initial ice and its subsequent

142 warming to room temperature. The formation of glycine in ice analog can occur following different pathways. It
 143 may occur through ice processing via the transformation of methyl carbamate into glycinate salt under UV
 144 irradiation (Figure 3A) ^{26,27}, as supported by the detection of methylamine in pre-accretional analogs ²⁸. No
 145 investigation has been conducted on the formation of the other three amino acids, making it difficult to propose
 146 hypotheses about their formation mechanism in such ices. The Strecker synthesis has been shown to occur
 147 partially during photo-processing and heating of ices, since its last step, which consists in the hydrolysis of the
 148 amino nitrile, is not possible in these conditions due to a high energy barrier ²⁹⁻³¹, which prevents the formation
 149 of glycine. Nonetheless, radical and thermal chemistries is likely to play an important role in their formation
 150 (Figure 3B) ^{32,33}.

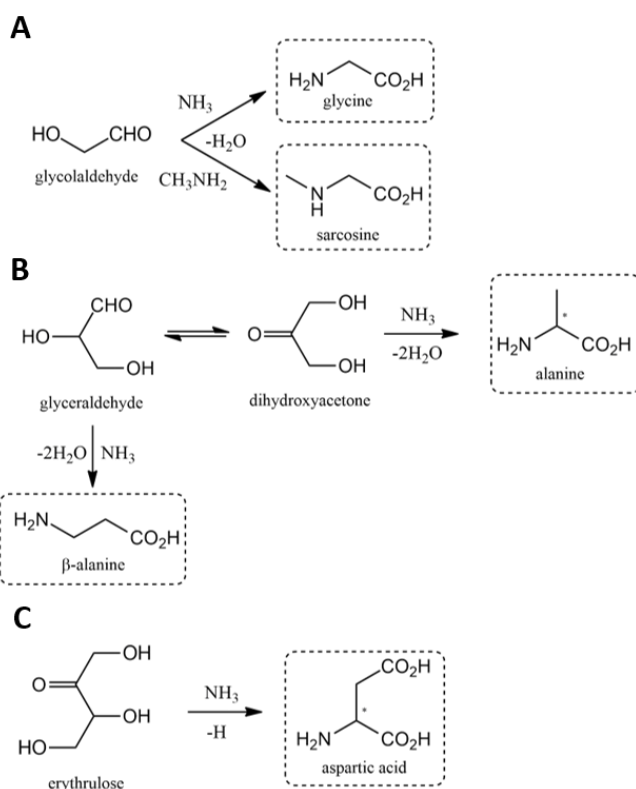


151

152 **Figure 3 – Potential chemical reactions occurring during the initial processing of interstellar ice analogs**
 153 **and leading to the formation of glycine formation. The reaction occurs at low temperature (77 K) and**
 154 **pressure (10⁻⁸ mbar) under UV irradiation at 121 nm.**

155 After incubating the analog in water at 150 °C, a rapid increase in amino acid abundances was observed, except
 156 for D-valine and D-leucine, which appear only after 30 days. If the Strecker synthesis would be involved in
 157 amino acid formation, the absence of valine and leucine within the first 30 days suggests that this process alone
 158 cannot explain the formation of α -amino acids. In addition to glycine, D-alanine, sarcosine, D-aspartic acid and
 159 β -alanine are also formed, which may be the result of the reaction of carbohydrates present in the analog ^{19,34-37}
 160 with ammonia or methylamine (Figure 4). This scenario is strengthened by kinetic profiles that show the
 161 involvement of carbohydrates in amino acid formation from a formaldehyde mixture at high temperatures ³⁸. A
 162 rapid increase of amino acid formation is also observed followed by a rapid decrease of amino acid abundance in
 163 the same time range as observed in our experiment. In this scenario, glycine and sarcosine can be formed from
 164 glycolaldehyde (Figure 4A) ³⁹, whereas β -alanine could arise from the reaction between glyceraldehyde and
 165 ammonia. D-alanine can be produced by isomerization of dihydroxyacetone, which reacts with ammonia (Figure
 166 4B). Aspartic acid can be formed by the reaction of ammonia with erythrulose (Figure 4C). D-2-ABA and D-3-
 167 ABA can be generated also from sugars or sugar acids ³⁸.

Phase ①



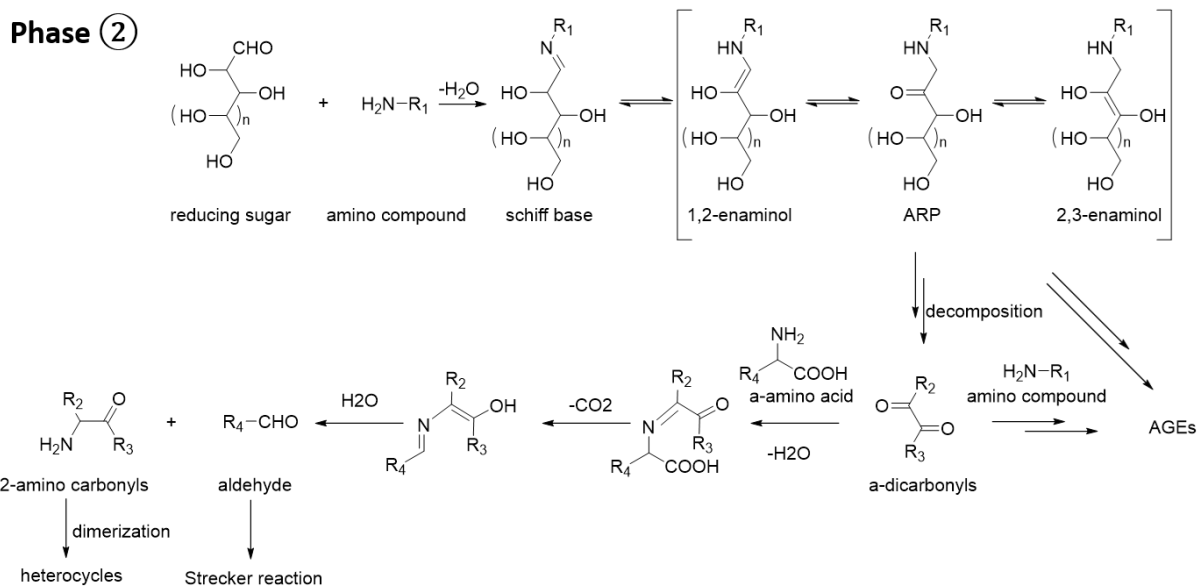
168

169 **Figure 4 – Potential chemical reactions leading to α - and β -amino acids during the early stages of**
 170 **incubating a pre-accretional analog in water at 150 °C.**

171 Following a 3-day incubation period (phase 2, Figure 2), there is a strong reduction in the abundance of amino
 172 acids, suggesting that the previous reservoir (phase 1, Figure 2) of amino acid precursors has been either
 173 consumed or destroyed. A such strong decrease cannot be explained only by amino acid degradation leading to
 174 CO_2 and NH_3 release^{38,40}. Reactions between amino acids and other compounds like urea⁴¹ can occur, leading to
 175 the formation of carbamoyl amino acids that give back amino acids^{42,43}. However, to explain this profile, a
 176 simultaneous consumption of amino acid precursors and amino acids may be required. A potential explanation
 177 would be the Maillard reaction (Figure 5), where amino acids react with sugars leading to the consumption of
 178 both amino acids and sugars⁴⁴.

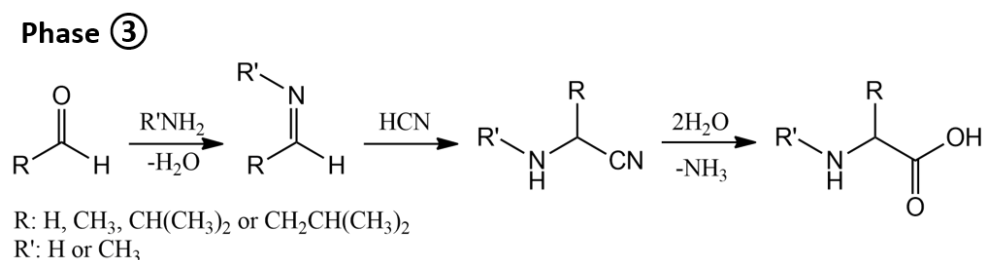
179 To verify this hypothesis, stoichiometric formula of products resulting from the Maillard reaction (Amadori
 180 product (ARP), Figure 5) where searched in high-resolution mass spectrometry data of the same samples (data
 181 published in Danger et al.²³). Table S1 shows the possible ARPs and their sum formulas based on the expected
 182 reaction between the experimentally found amino acids (alanine/sarcosine, glycine, aspartic acid, valine, leucine,
 183 2-ABA, 3-ABA) and reducing sugars with basic CH_2O unit from 2 to 6. All potential formulas were found in the
 184 experimental data during all the hydrothermal process. ARPs are already present in non-negligible amounts in
 185 the original pre-accretional analog that was conserved at -30°C (Figure S5). Keeping the original sample in water
 186 at cold temperature (5°C) changed slightly the concentration of the ARPs, some being degraded, others being
 187 produced. The kinetic from 1 day to 100 days at 150°C showed a combined effect of (i) disappearance of the
 188 ARPs, further engaged in reactions and (ii) further reactivity of the amino acids with reducing sugars in heated
 189 solution, following Maillard reactions and leading to the same ARP. At the beginning of the reaction, the
 190 hydrothermal process generated more ARPs, due to the reaction of the amino acids with the present reducing
 191 sugars (Figure S6). Interestingly, the profiles of the ARPs follow the profiles of the amino acid concentration in
 192 the first 30 days of the process in similar phases 1, 2, 3 and confirm the differential kinetics in the formation of
 193 novel amino acids via the Strecker reaction and their relative consumption and successive formation of ARPs via
 194 the Maillard hydrothermal reaction. After 30 days of processing, the formation of ARPs decreased due to the
 195 limited availability of precursor-reducing sugar. As the degradation of ARPs continued, their intensity kept
 196 decreasing. It has to be noted, that while with GC-FT-OrbitrapMS analyses, valine is not detected, FT-ICR-MS

197 analyses suggest the formation of its ARP product at low duration, which is not the case for leucine. It seems that
 198 valine is also present in the initial pre-accretional analog.



199
 200 **Figure 5 – Maillard reaction may lead to amino compound degradation during Phase 2 with incubation of**
 201 **a pre-accretional analog in water at 150 °C. Reducing sugar can react with the amine group of amino**
 202 **compounds to form a Schiff base, followed by the Amadori rearrangement to an Amadori product (ARP).**
 203 **Decomposition of ARP by fragmentation of the carbohydrate backbone can generate various α -**
 204 **dicarbonyls. Only α -amino acids can undergo α -dicarbonyls-assisted oxidative decarboxylation and form**
 205 **aldehydes, which could form some α -amino acids at Phase 3 by Strecker reaction. α -dicarbonyls can also**
 206 **react with amino compounds to produce stable advanced glycation end products (AGEs).**

207 After ten days of incubation, a new evolution of amino acid formation occurs. This phase 3 is characterized by
 208 the formation of only α -amino acids, including glycine, D-alanine, D-2-ABA, sarcosine, D-valine and D-leucine,
 209 while D-aspartic acid disappears completely, along with β -amino acids (β -alanine and D-3-ABA). This implies a
 210 chemical reaction specific to the formation of aliphatic α -amino acids, such as the Strecker synthesis (Figure 6),
 211 which is known to produce α -amino acids during aqueous alteration in meteorite's parent bodies^{45,5}. During the
 212 first days of incubation, the aqueous alteration causes a transformation of the initial molecules of the pre-
 213 accretional analog²³, leading to the formation of aldehydes, NH_3 and HCN into the aqueous environment. As
 214 previously noted, some aldehydes may be formed from Strecker degradation or Amadori rearrangement products^{46,47}
 215 of the Maillard reaction occurring in Phase 2 (Figure 5). Aspartic acid is not formed after ten days, which
 216 indicates that its aldehyde precursor is not available or that aspartic acid is present at a concentration below our
 217 detection limit. Different intensity profiles are observed for α -amino acids, with D-valine and D-leucine showing
 218 a decrease in abundances after 30 days of reaction, while other α -amino acids continue to rise. This could be due
 219 to the limited availability of aldehyde precursors for valine and leucine compared to formaldehyde and
 220 acetaldehyde for glycine and alanine, respectively. Generally, the formation of aldehydes and their precursors
 221 from the initial ice photo-processing involves free-radical chemistry, which leads to a decrease in compound
 222 abundance with an increase in carbon number and ramification⁴⁸. Therefore, the initial abundance of more
 223 complex aldehydes and their corresponding amino acids is expected to be lower than that of simpler α -amino
 224 acids.



226 **Figure 6 – Strecker reaction likely occurring during phase 3, resulting in the formation of only α -amino**
227 **acids.**

228 A fraction of the precursors of organic matter found in carbonaceous chondrites is believed to originate from
229 dense molecular cloud ices^{49–51}. This scenario is strengthened by analyses of samples returned from the Ryugu
230 asteroid⁴. However, the present experiments demonstrate that these ices can only generate a limited diversity
231 and quantity of amino acids due to insufficient available energy. Investigations into the Strecker synthesis of α -
232 amino acids from these ices has demonstrated this limitation^{31,52–54}. Therefore, by considering only ices, the total
233 amount of amino acids incorporated inside parent bodies of carbonaceous chondrites is expected to be low.
234 Nonetheless, one must emphasize that the high molecular diversity generated during the ice processing present
235 numerous amino acid precursors^{19,48,55}, next to others sources of amino acids possibly present in the disk.

236 This pre-accretional organic matter is highly reactive and is susceptible to undergo a secondary evolution inside
237 meteorite parent bodies, as shown by laboratory experiments⁵⁶. Meteorite analyses have indeed demonstrated
238 that aqueous alteration has occurred within their parent bodies^{57–60}, a fact confirmed by the analyses of samples
239 returned from the Ryugu asteroid^{4,61}. As shown in this work, when a pre-accretional organic analog is placed in
240 water according to this alteration scenario, its molecular diversity evolve²³ and leads to the formation of
241 numerous amino acids, with increasing formation rates as the temperature increases. Furthermore, depending on
242 the time of aqueous alteration, different chemical pathways occur leading to variation in abundances and types of
243 amino acids. Other targeted analyses on amino acids on similar analogs altered at 125 °C showed also weak
244 evolution of several amino acids²⁸. The concentration of α -amino acids (glycine, alanine and serine) tends to
245 increase with time, while the concentration of β -alanine decreases. Trends observed in Qasim et al. are less
246 pronounced than in our experiment, probably because of the differences of experimental conditions compared to
247 our conditions, since they use lower temperatures (125 °C vs. 150 °C) and lower duration experiments (30 days
248 vs. 100 days). In this evolution, sugars play an important role in amino acid formation at short durations or low
249 temperatures, as shown here, whereas the Strecker synthesis plays this role at longer durations. Since amino acid
250 precursors differ between these two reactions, the amino acids finally formed differ in content and amount. At
251 short reaction times, small α -amino acids (glycine, alanine, sarcosine, 2-ABA) are formed, along with β -amino
252 acids (β -alanine, 3-ABA). At longer durations, β -amino acids disappear entirely, and more complex α -amino
253 acids are formed. Further experiments are needed to monitor the evolution of sugars in order to compare it with
254 the evolution of amino acids to definitively validate this scheme. The present experiment indicates that the
255 complexity of amino acids observed in carbonaceous meteorites and asteroids probably originated from
256 secondary processing, and not directly from the ice chemistry, and depends on the molecular diversity generated
257 from the initial ice. The formation of amino acids in such object is thus related to a complex chemical network
258 has observed in our present experimental work.

259 However, the laboratory study of the evolution of the pre-accretional analog in an aqueous environment suggests
260 that a higher presence of β -amino acids should indicate a lower aqueous alteration, while a higher presence of α -
261 amino acids on longer alteration period. For instance, higher β -alanine/glycine are observed at lower degree of
262 alteration of pre-accretional analogs (Table 1). This finding is corroborated by similar aqueous alteration
263 experiments performed by Qasim *et al.*²⁸ on a similar pre-accretional material. At the contrary, in meteorites, it
264 is proposed that lower degree of aqueous alteration favors the presence of α -amino acids via the Strecker
265 synthesis, while higher degree of alteration enhances the presence of β -amino acids compared to α -amino acids
266^{21,62,63}. Therefore, higher β -alanine/glycine ratios are observed for more aqueous altered meteorite. These
267 discrepancies could be due to factors as the influence of minerals (absent in our experiments), different alteration
268 timeframes, or additional origins of amino acids or their precursors. Further experiments have to explore these
269 hypotheses.

270 **4. MATERIAL AND METHODS**

271 **4.1 Chemicals and solutions**

272 For amino acid analyses, each amino acid standard was prepared individually and then mixed together in 0.1 M
273 hydrochloric acid (HCl) to obtain a stock solution of 10^{-4} M. Serial dilutions were prepared for calibration
274 curves. The 0.1 M HCl solution was prepared by diluting 6N HCl (specific ampoule for amino acid analysis,
275 Merck) in ultra-pure water produced by a Direct-Q® 3 UV water purification system. All amino acids and

276 chemicals used were from Sigma-Aldrich, Fluka, or Acros Organics. For more information see Garcia et al. 2023
277 ²⁵.

278 4.2 Derivatization procedure

279 Amino acid solutions were derivatized into their *N* (*O*, *S*)-ethoxy-carbonylheptafluorobutylester (ECHFBFBE)
280 derivatives according to the protocol developed by Meinert et al. ⁶⁴. In a conical reaction flask (Reactival,
281 Thermo Scientific™), a 10 μL volume of aqueous amino acid solution in 0.1 M HCl reacted with 3.8 μL of
282 2,2,3,3,4,4,4-heptafluoro-1-butanol and 1.2 μL of pyridine. After 15 s of stirring, 1 μL of ethyl chloroformate
283 were added and the resulting solution stirred vigorously for 15 seconds. The ECHFBFBE derivatives were extracted
284 with 10 μL of a 10⁻⁵ M methyl laurate (internal standard) chloroform solution. The organic phase containing the
285 ECHFBFBE derivatives was then transferred into 1 mL GC vials equipped with 100 μL inserts for GC-FT-
286 Orbitrap-MS analysis. Note that this derivatization method does not provide identical yields among different
287 amino acid groups, especially discriminating α, α-dialkyl amino acids as well as γ-amino acids ^{25,65}. Each sample
288 was injected in triplicate to obtain information on the instrument repeatability.

289 4.3 Post-analysis data processing

290 All data were acquired in TIC and processed with Qual Browser Xcalibur. For each amino acid, the search and
291 identification was performed by mass extraction, based on the retention time and a specific mass/charge ratio
292 (*m/z*) for each amino acid (amino acid databases ²⁵). The monitoring of amino acid profiles was performed by
293 integrating the characteristic ion of each amino acid *A*(*x*) divided by the integrated area of the internal standard
294 *A*(IS), *A*(*x*)/*A*(IS). To correct for possible contamination, the values obtained were subtracted from a
295 derivatization blank, which consists in 0.1 M HCl solvent used for the dilution of the amino acids, to which the
296 derivatization step was applied. Corrected data result in *A*(*x*)/*A*(IS)-*A*(*x*)_b/*A*(IS)_b. Only concentrations of amino
297 acids that are equal or above the quantification limit are indicated ²⁵, while amino acids whose values are
298 between detection and quantification limits are only indicated as identified.

299 4.4 Synthesis of pre-accretional organic analogs to post-accretional organic material

300 A pre-accretional organic analog was formed from an ice including H₂O, ¹²CH₃OH and NH₃ in proportion of
301 3:1:1. The corresponding gas mixture was deposited in a stainless steel chamber on a copper cold finger at low
302 pressure (10⁻⁷ to 10⁻⁸ mbar) and low temperature (77 K) forming an ice, analog to the ones observed in dense
303 molecular clouds on silicate grains⁶⁶. The ice formation was concomitant to its irradiation with a dihydrogen UV
304 microwave discharge lamp (mainly emitting at 121 nm) to simulate stellar radiation. After 72 h of deposition and
305 simultaneous irradiation, the photo-processed ice was slowly heated to 300 K to obtain an analog of pre-
306 accretional organic matter. Aqueous alteration experiments were conducted with 100 μL of the pre-accretional
307 analog dissolved in milli-Q water at a concentration of 1 g L⁻¹ (more details in Danger et al. 2021 ²³). Sealed
308 gold capsules were held at 5 °C (100 days) or 150 °C for varying length of time (1, 3, 10, 30 and 100 days). The
309 pressure inside the reactors was not monitored and should correspond to the vapor pressure of water, i.e. up to 5
310 bars at 150 °C. At the end of the experiments, 10 μL of the 100 μL solution was used for amino acid analyses
311 following the procedure described in section 2.2. Furthermore, one fraction of the initial pre-accretional analogue
312 solution was dried and stored at -30 °C and directly converted into ECHFBFBE derivatives forming the non-altered
313 sample. Another fraction was recovered in 6N HCl to be hydrolyzed during 24 h at 110 °C followed by the
314 ECHFBFBE derivatization.

315 4.5 GC-FT-Orbitrap-MS configuration

316 Analyses were performed on a Trace 1310 gas chromatograph (GC) coupled to a Q-Exactive Orbitrap™ mass
317 spectrometer (MS) from Thermo Fisher Scientific operated at PIIM. Injections were performed with an auto-
318 sampler (AI 1310 from Thermo Fisher) in splitless mode (splitless time: 1 min) with an injector temperature of
319 230 °C. Helium was used as carrier gas with a flow rate of 1 mL min⁻¹ and a purge rate of 5.0 mL min⁻¹.
320 Amino acids were separated on two Chirasil-L-Val columns (each 25 m x 0.25 mm x 0.12 μm film thickness,
321 Agilent) connected with a Valco connector. The duration of the oven temperature program was 90 min with a
322 solvent delay of 14 min. The optimized temperature program was as follows: 40 °C for 1 min, then increased to
323 80 °C with a slope of 10 °C min⁻¹ during 10 min then 2 °C min⁻¹ to reach 190 °C with an isotherm during 20
324 min. The transfer line was set at 250 °C. The *m/z* range was 50–400 with a FWHM resolution fixed at 60 000, a
325 target AGC value at 10⁶ and a max IT at 200 ms. Electron impact ionization was used at 70 eV.

327 **Acknowledgement**

328 The research was funded by the Centre National d'Etudes Spatiales (CNES, R-S18/SU-0003-072 and R-S18/SU-
 329 0003-072, PI: G. D.), and the Centre National de la Recherche Française (CNRS) with the programs "Physique
 330 et Chimie du Milieu Interstellaire" (PCMI-PI:G.D.) and "Programme National de Planétologie" (PNP) (PI:
 331 G.D.). G.D is grateful to the Agence Nationale de la Recherche for funding via the ANR RAHIA_SSOM
 332 (ANR-16-CE29-0015) and VAHIA (ANR-12-JS08-0001). The project has further received funding from the
 333 EXCellence Initiative of Aix-Marseille Université - A*Midex, a French "Investissements d'Avenir programme"
 334 AMX-21-IET-018, from the Région SUD Provence Alpes Côte d'Azur "Apog 2017" – PILSE, as well by the EU
 335 Framework Program for Research and Innovation Horizon 2020 (grants ERC 804144, ALIFE). L.R. thanks the
 336 European Research Council for funding via the ERC project HYDROMA (grant agreement No. 819587).

337 **Reference**

- 338 1. Caselli, P. & Ceccarelli, C. Our astrochemical heritage. *Astron. Astrophys. Rev.* **20**, 56 (2012).
- 339 2. Pizzarello, S., Yarnes, C. T. & Cooper, G. The Aguas Zarcas (CM2) meteorite: New insights into early
 340 solar system organic chemistry. *Meteorit. Planet. Sci.* **14**, maps.13532 (2020).
- 341 3. Beth, A. *et al.* ROSINA ion zoo at Comet 67P. *Astron. Astrophys.* 1–26 (2020) doi:10.1051/0004-
 342 6361/201936775.
- 343 4. Naraoka, H. *et al.* Soluble organic molecules in samples of the carbonaceous asteroid (162173) Ryugu.
 344 *Science (80-.)*. **379**, (2023).
- 345 5. Sakaguchi, C. *et al.* Insights into the formation and evolution of extraterrestrial amino acids from the
 346 asteroid Ryugu. *Nat. Commun.* **14**, 1482 (2023).
- 347 6. Oba, Y. *et al.* Uracil in the carbonaceous asteroid (162173) Ryugu. *Nat. Commun.* **14**, 1292 (2023).
- 348 7. Abreu, N. M., Aponte, J. C., Cloutis, E. A. & Nguyen, A. N. The Renazzo-like carbonaceous chondrites
 349 as resources to understand the origin, evolution, and exploration of the solar system. *Geochemistry* **80**,
 350 125631 (2020).
- 351 8. Schmitt-Kopplin, P. *et al.* High molecular diversity of extraterrestrial organic matter in Murchison
 352 meteorite revealed 40 years after its fall. *Proc. Natl. Acad. Sci. U. S. A.* **107**, 2763–2768 (2010).
- 353 9. Danger, G. *et al.* Unprecedented Molecular Diversity Revealed in Meteoritic Insoluble Organic Matter:
 354 The Paris Meteorite's Case. *Planet. Sci. J.* **1**, 55 (2020).
- 355 10. Pizzarello, S.; Cooper, G. W.; Flynn, G. J. The Nature and Distribution of the Organic Material in
 356 Carbonaceous Chondrites and Interplanetary Dust Particles. in *Meteorites and the Early Solar System II*
 357 p.625-651 (2006).
- 358 11. Callahan, M. P. *et al.* Carbonaceous meteorites contain a wide range of extraterrestrial nucleobases.
 359 *Proc. Natl. Acad. Sci. U. S. A.* **108**, 13995–13998 (2011).
- 360 12. Furukawa, Y. *et al.* Extraterrestrial ribose and other sugars in primitive meteorites. *Proc. Natl. Acad. Sci.*
 361 **116**, 24440–24445 (2019).
- 362 13. Lecasble, M., Remusat, L., Viennet, J.-C., Laurent, B. & Bernard, S. Polycyclic aromatic hydrocarbons
 363 in carbonaceous chondrites can be used as tracers of both pre-accretion and secondary processes.
 364 *Geochim. Cosmochim. Acta* **335**, 243–255 (2022).
- 365 14. Elsila, J. E. *et al.* Meteoritic Amino Acids: Diversity in Compositions Reflects Parent Body Histories.
 366 *ACS Cent. Sci.* acscentsci.6b00074 (2016) doi:10.1021/acscentsci.6b00074.
- 367 15. Burton, A. S., Stern, J. C., Elsila, J. E., Glavin, D. P. & Dworkin, J. P. Understanding prebiotic
 368 chemistry through the analysis of extraterrestrial amino acids and nucleobases in meteorites. *Chem. Soc.*
 369 *Rev.* **41**, 5459–72 (2012).
- 370 16. Danger, G. *et al.* Characterization of laboratory analogs of interstellar/cometary organic residues using
 371 very high resolution mass spectrometry. *Geochim. Cosmochim. Acta* **118**, 184–201 (2013).

- 372 17. Ruf, A. *et al.* The Challenging Detection of Nucleobases from Pre-accretional Astrophysical Ice
373 Analogs. *Astrophys. J. Lett.* **887**, L31 (2019).
- 374 18. Oba, Y., Takano, Y., Naraoka, H., Watanabe, N. & Kouchi, A. Nucleobase synthesis in interstellar ices.
375 *Nat. Commun.* **10**, 4413 (2019).
- 376 19. Meinert, C. *et al.* Ribose and related sugars from ultraviolet irradiation of interstellar ice analogs.
377 *Science (80-.)*. **352**, 208–212 (2016).
- 378 20. Muñoz Caro, G. M. *et al.* Amino acids from ultraviolet irradiation of interstellar ice analogues. *Nature*
379 **416**, 403–406 (2002).
- 380 21. Modica, P., Martins, Z., Meinert, C., Zanda, B. & d’Hendecourt, L. L. S. The Amino Acid Distribution
381 in Laboratory Analogs of Extraterrestrial Organic Matter: A Comparison to CM Chondrites. *Astrophys.*
382 *J.* **865**, 41 (2018).
- 383 22. Danger, G. *et al.* The transition from soluble to insoluble organic matter in interstellar ice analogs and
384 meteorites. *Astron. Astrophys.* (2022) doi:10.1051/0004-6361/202244191.
- 385 23. Danger, G. *et al.* Exploring the link between molecular cloud ices and chondritic organic matter in
386 laboratory. *Nat. Commun.* **12**, 1–9 (2021).
- 387 24. Danger, G. *et al.* Insight into the molecular composition of laboratory organic residues produced from
388 interstellar/pre-cometary ice analogues using very high resolution mass spectrometry. *Geochim.*
389 *Cosmochim. Acta* **189**, 184–196 (2016).
- 390 25. Garcia, A. *et al.* Gas chromatography coupled-to Fourier transform orbitrap mass spectrometer for
391 enantioselective amino acid analyses: Application to pre-cometary organic analog. *J. Chromatogr. A*
392 **1704**, 464118 (2023).
- 393 26. Bossa, J. B. *et al.* Methylammonium methylcarbamate thermal formation in interstellar ice analogs: a
394 glycine salt precursor in protostellar environments. *Astron. Astrophys.* **506**, 601–608 (2009).
- 395 27. Bossa, J. B., Borget, F., Duvernay, F., Theulé, P. & Chiavassa, T. How a usual carbamate can become an
396 unusual intermediate: a new chemical pathway to form glycinate in the interstellar medium. *J. Phys.*
397 *Org. Chem.* **23**, 333–339 (2010).
- 398 28. Qasim, D. *et al.* Meteorite Parent Body Aqueous Alteration Simulations of Interstellar Residue Analogs.
399 *ACS Earth Sp. Chem.* (2023) doi:10.1021/acsearthspacechem.2c00274.
- 400 29. Singh, S. K., Zhu, C., La Jeunesse, J., Fortenberry, R. C. & Kaiser, R. I. Experimental identification of
401 aminomethanol (NH₂CH₂OH)—the key intermediate in the Strecker Synthesis. *Nat. Commun.* **13**, 375
402 (2022).
- 403 30. Danger, G. *et al.* Experimental investigation of aminoacetonitrile formation through the Strecker
404 synthesis in astrophysical-like conditions: Reactivity of methanimine (CH₂=NH), ammonia
405 (NH₃), and hydrogen cyanide (HCN). *Astron. Astrophys.* **535**, (2011).
- 406 31. Danger, G., Duvernay, F., Theule, P., Borget, F. & Chiavassa, T. Hydroxyacetonitrile (HOCH₂CN)
407 Formation In Astrophysical Conditions. Competition With The Aminomethanol, A Glycine Precursor.
408 *Astrophys. J.* **756**, 11 (2012).
- 409 32. Holtom, P. D., Bennett, C. J., Osamura, Y., Mason, N. J. & Kaiser, R. I. A combined experimental and
410 theoretical study on the formation of the amino acid glycine (NH₂CH₂COOH) and its isomer
411 (CH₃NHCOOH) in extraterrestrial ices. *Astrophys. J.* **626**, 940–952 (2005).
- 412 33. Theule, P. *et al.* Thermal reactions in interstellar ice: a step towards molecular complexity in the
413 interstellar medium. *Adv. Sp. Res.* **52**, 1567–1579 (2013).
- 414 34. Layssac, Y., Gutiérrez-Quintanilla, A., Chiavassa, T. & Duvernay, F. Detection of glyceraldehyde and
415 glycerol in VUV processed interstellar ice analogues containing formaldehyde: a general formation route
416 for sugars and polyols. *Mon. Not. R. Astron. Soc.* **496**, 5292–5307 (2020).
- 417 35. Kebukawa, Y., Chan, Q. H. S., Tachibana, S., Kobayashi, K. & Zolensky, M. E. One-pot synthesis of
418 amino acid precursors with insoluble organic matter in planetesimals with aqueous activity. *Sci. Adv.* **3**,
419 e1602093 (2017).

- 420 36. Vinogradoff, V. *et al.* Impact of Phyllosilicates on Amino Acid Formation under Asteroidal Conditions. *ACS Earth Sp. Chem.* **4**, 1398–1407 (2020).
421
- 422 37. Koga, T. & Naraoka, H. Synthesis of Amino Acids from Aldehydes and Ammonia: Implications for
423 Organic Reactions in Carbonaceous Chondrite Parent Bodies. *ACS Earth Sp. Chem.* **6**, 1311–1320
424 (2022).
- 425 38. Aubrey, A. D., Cleaves, H. J. & Bada, J. L. The Role of Submarine Hydrothermal Systems in the
426 Synthesis of Amino Acids. *Orig. Life Evol. Biosph.* **39**, 91–108 (2009).
- 427 39. YANAGAWA, H., Kobayashi, Y. & Egami, F. Genesis of Amino Acids in the Primeval Sea. *J. Biochem*
428 **87**, 359–362 (1980).
- 429 40. Körner, P. Hydrothermal Degradation of Amino Acids. *ChemSusChem* **14**, 4947–4957 (2021).
- 430 41. Nuevo, M. *et al.* Urea, glycolic acid, and glycerol in an organic residue produced by ultraviolet
431 irradiation of interstellar/pre-cometary ice analogs. *...Astrobiology* **10**, 245–256 (2010).
- 432 42. Danger, G., Boiteau, L., Cottet, H. & Pascal, R. The peptide formation mediated by cyanate revisited. N-
433 carboxyanhydrides as accessible intermediates in the decomposition of N-carbamoylamino acids. *J. Am.*
434 *Chem. Soc.* **128**, 7412–7413 (2006).
- 435 43. Danger, G., Plasson, R. & Pascal, R. Pathways for the formation and evolution of peptides in prebiotic
436 environments. *Chem. Soc. Rev.* **41**, 5416–5429 (2012).
- 437 44. Hemmler, D. *et al.* Evolution of Complex Maillard Chemical Reactions, Resolved in Time. *Sci. Rep.* **7**,
438 3–8 (2017).
- 439 45. Elsila, J. E., Dworkin, J. P., Bernstein, M. P., Martin, M. P. & Sandford, S. A. Mechanisms of amino
440 acid formation in interstellar ice analogs. *Astrophys. J.* **660**, 911–918 (2007).
- 441 46. YAYLAYAN, V. A. Recent Advances in the Chemistry of Strecker Degradation and Amadori
442 Rearrangement: Implications to Aroma and Color Formation. *Food Sci. Technol. Res.* **9**, 1–6 (2003).
- 443 47. Davidek, T., Clety, N., Aubin, S. & Blank, I. Degradation of the Amadori Compound N-(1-Deoxy-d-
444 fructos-1-yl)glycine in Aqueous Model Systems. *J. Agric. Food Chem.* **50**, 5472–5479 (2002).
- 445 48. Abou Mrad, N., Duverney, F., Chiavassa, T. & Danger, G. Methanol ice VUV photo-processing: GC-
446 MS analysis of volatile organic compounds. *Mon. Not. R. Astron. Soc.* **458**, 1234–1241 (2016).
- 447 49. Le Guillou, C., Bernard, S., Brearley, A. J. & Remusat, L. Evolution of organic matter in Orgueil,
448 Murchison and Renazzo during parent body aqueous alteration: In situ investigations. *Geochim.*
449 *Cosmochim. Acta* **131**, 368–392 (2014).
- 450 50. Le Guillou, C. & Brearley, A. Relationships between organics, water and early stages of aqueous
451 alteration in the pristine CR3.0 chondrite MET 00426. *Geochim. Cosmochim. Acta* **131**, 344–367 (2014).
- 452 51. Vinogradoff, V. *et al.* Paris vs. Murchison: Impact of hydrothermal alteration on organic matter in CM
453 chondrites. *Geochim. Cosmochim. Acta* **212**, 234–252 (2017).
- 454 52. Fresneau, A. *et al.* Thermal formation of hydroxynitriles, precursors of hydroxyacids in astrophysical
455 ice analogs: Acetone ($(\text{CH}_3)_2\text{C}=\text{O}$) and hydrogen cyanide (HCN) reactivity. *Mol. Astrophys.* **1**,
456 1–12 (2015).
- 457 53. Danger, G. *et al.* Experimental investigation of aminoacetonitrile formation through the Strecker
458 synthesis in astrophysical-like conditions: reactivity of methanimine (CH_2NH), ammonia (NH_3), and
459 hydrogen cyanide (HCN). *Astron. Astrophys.* **535**, A47 (2011).
- 460 54. Fresneau, A. *et al.* Ice chemistry of acetaldehyde reveals competitive reactions in the first step of the
461 Strecker synthesis of alanine: formation of $\text{HO}-\text{CH}(\text{CH}_3)-\text{NH}_2$ vs. $\text{HO}-\text{CH}(\text{CH}_3)-\text{CN}$. *Mon.*
462 *Not. R. Astron. Soc.* **1660**, 1649–1660 (2015).
- 463 55. Vinogradoff, V. *et al.* New insight into the formation of hexamethylenetetramine (HMT) in interstellar
464 and cometary ice analogs. *Astron. Astrophys.* **530**, A128 (2011).
- 465 56. Danger, G. *et al.* Exploring the link between molecular cloud ices and chondritic organic matter in

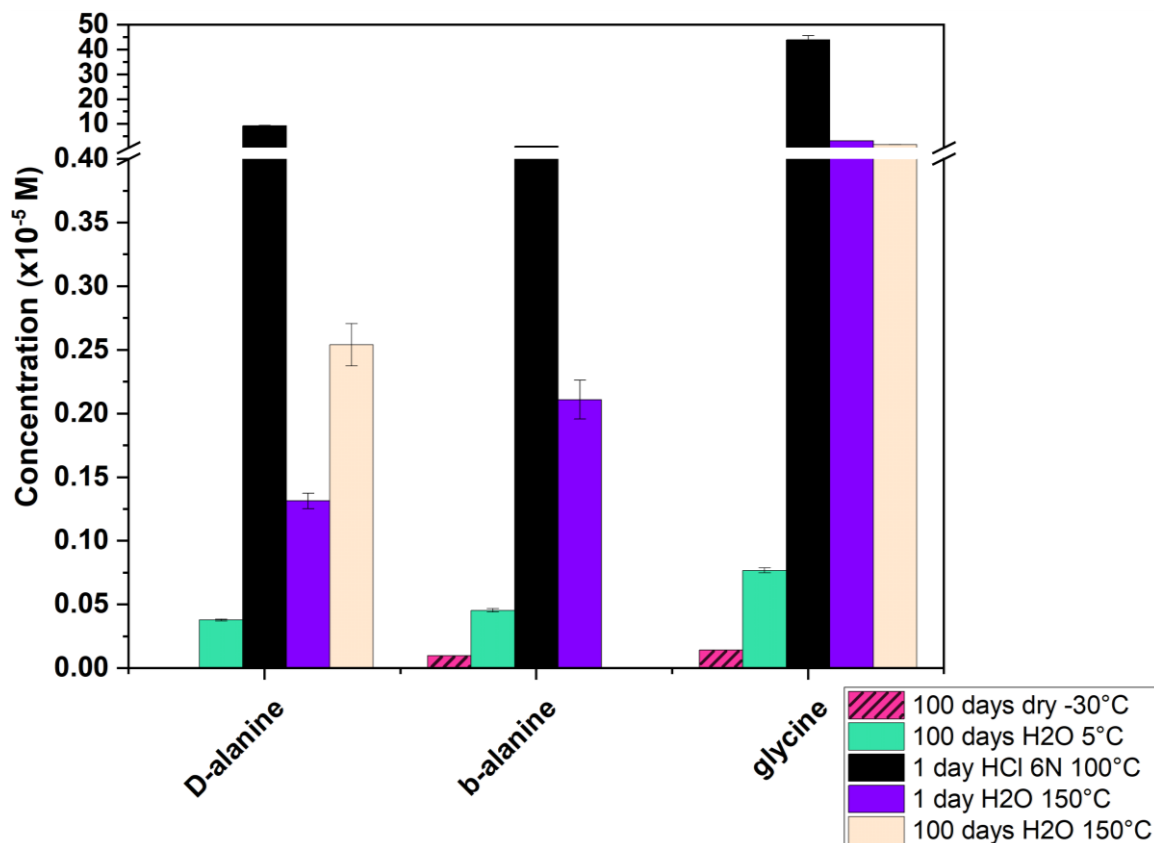
- 466 laboratory. *Nat. Commun.* **12**, 3538 (2021).
- 467 57. Glavin, D. P. *et al.* *The Origin and Evolution of Organic Matter in Carbonaceous Chondrites and Links*
468 *to Their Parent Bodies. Primitive Meteorites and Asteroids* (Elsevier Inc., 2018). doi:10.1016/B978-0-
469 12-813325-5.00003-3.
- 470 58. Suttle, M. D. *et al.* Alteration conditions on the CM and CV parent bodies – Insights from hydrothermal
471 experiments with the CO chondrite Kainsaz. *Geochim. Cosmochim. Acta* **318**, 83–111 (2022).
- 472 59. Jilly-Rehak, C. E., Huss, G. R., Nagashima, K. & Schrader, D. L. Low-Temperature Aqueous Alteration
473 on the Cr Chondrite Parent Body: Implications From in Situ Oxygen-Isotope Analyses. *Geochim.*
474 *Cosmochim. Acta* **222**, 230–252 (2017).
- 475 60. Brearley, A. J. The Action of Water. *Meteorites Early Sol. Syst. II* **943**, 587–624 (2006).
- 476 61. Nakamura, T. *et al.* Formation and evolution of carbonaceous asteroid Ryugu: Direct evidence from
477 returned samples. *Science (80-.)*. **379**, (2023).
- 478 62. Martins, Z., Modica, P., Zanda, B. & d’Hendecourt, L. L. S. The amino acid and hydrocarbon contents
479 of the paris meteorite: Insights into the most primitive cm chondrite. *Meteorit. Planet. Sci.* **50**, 926–943
480 (2015).
- 481 63. Burton, A. S., Grunsfeld, S., Elsila, J. E., Glavin, D. P. & Dworkin, J. P. The effects of parent-body
482 hydrothermal heating on amino acid abundances in CI-like chondrites. *Polar Sci.* **8**, 255–263 (2014).
- 483 64. Meinert, C. & Meierhenrich, U. J. Derivatization and Multidimensional Gas-Chromatographic
484 Resolution of α -Alkyl and α -Dialkyl Amino Acid Enantiomers. *Chempluschem* **79**, 781–785 (2014).
- 485 65. Myrgorodska, I., Meinert, C., Martins, Z., le Sergeant d’Hendecourt, L. & Meierhenrich, U. J.
486 Quantitative enantioseparation of amino acids by comprehensive two-dimensional gas chromatography
487 applied to non-terrestrial samples. *J. Chromatogr. A* **1433**, 131–136 (2016).
- 488 66. d’Hendecourt, L. & Dartois, E. Interstellar matrices: the chemical composition and evolution of
489 interstellar ices as observed by ISO . *Spectrochim. Acta. A* **57**, 669–684 (2001).

490

491 **FIGURES AND TABLES**

492

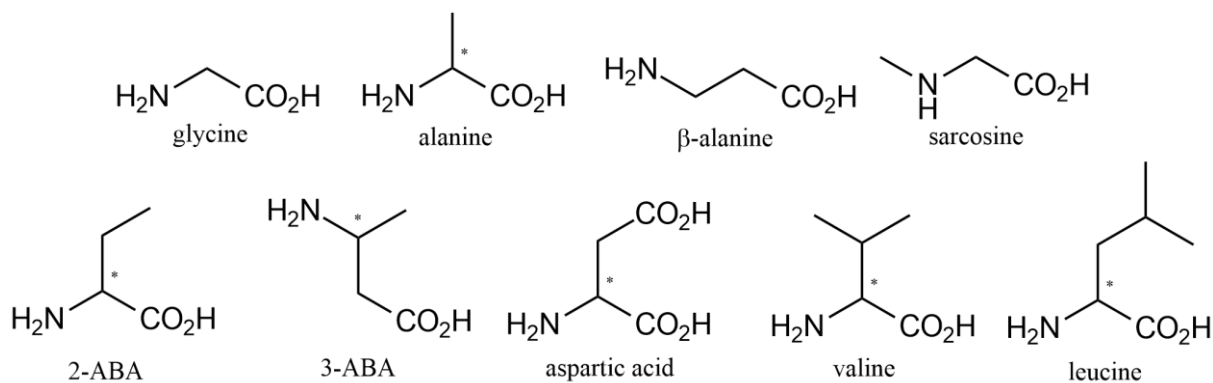
493 **Supplementary Information**



494

495 **Figure S1 – Concentration of D-alanine, β-alanine and glycine after 1 day in water at 150 °C or in HCl 6N**
 496 **at 110 °C compared to data displayed in Figure 1 for the initial pre-accretional analog (stored at -30°C in**
 497 **dry condition), and after 100 days in water at 5 °C or 150 °C. β-alanine and glycine in the pre-accretional**
 498 **analog (dry at -30 °C) are dashed because observed but below the quantification limit.**

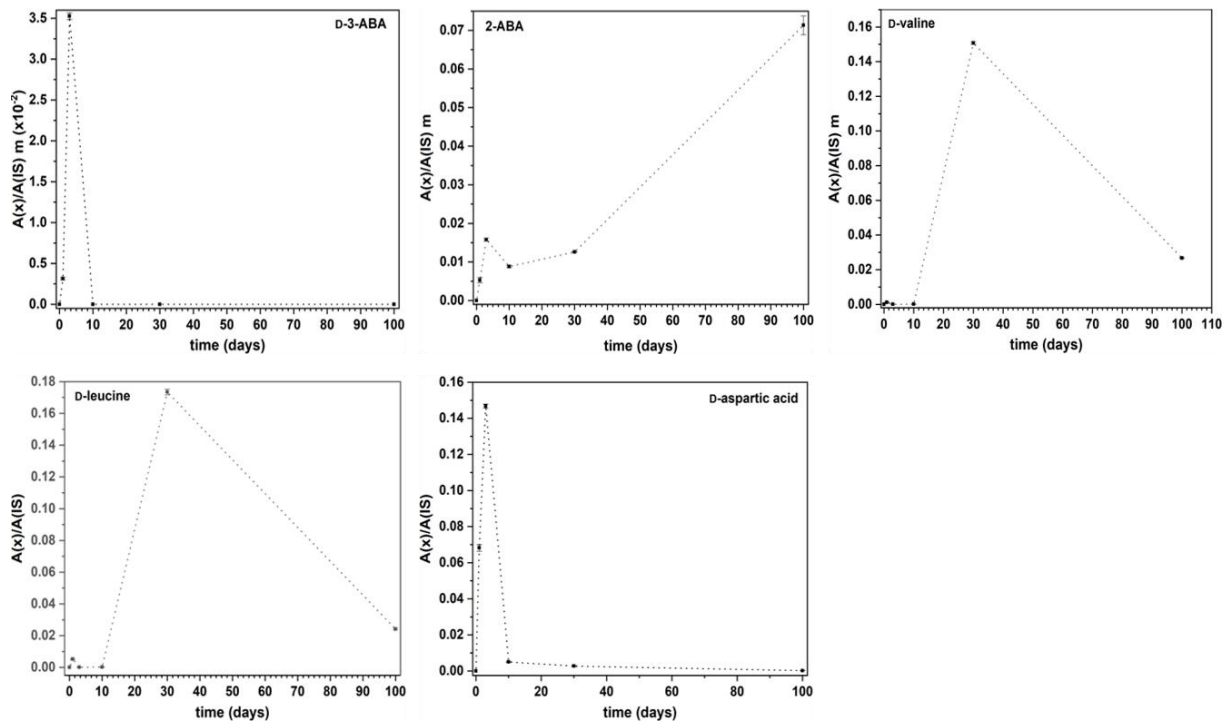
499



500

501 **Figure S2 – Amino acid structures observed in the different experiments to estimate the impact of aqueous**
 502 **alteration on the content and evolution of amino acids in a pre-accretional analogue.**

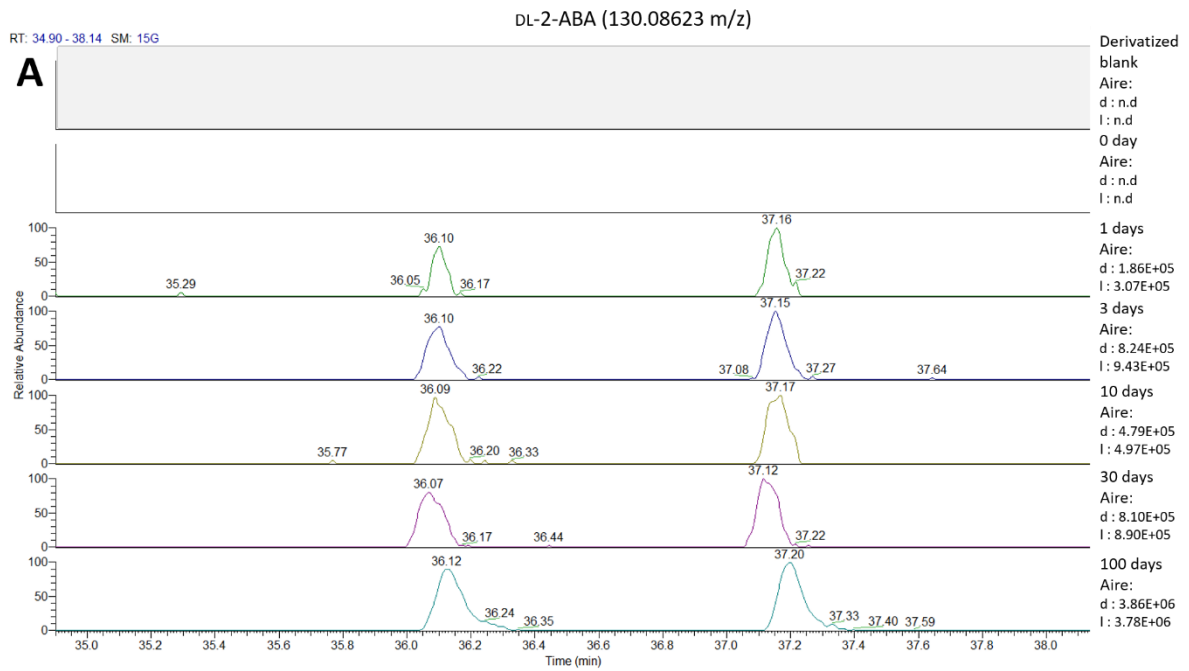
503



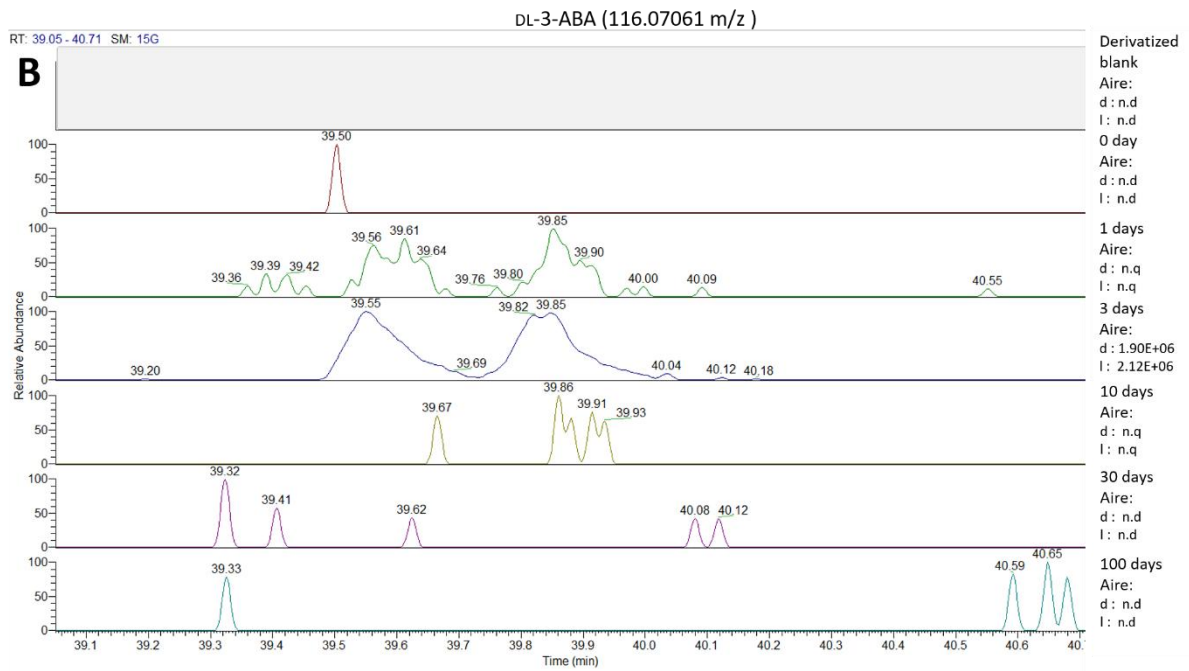
504

505 **Figure S3 – Monitoring of relative intensities of integrated areas of sample (amino acids, $A(x)$) against**
 506 **internal standard ($A(S)$) for several amino acids in a pre-accretional analogue incubated at 150 °C in**
 507 **water. The curves are only intended to serve as a visual guide.**

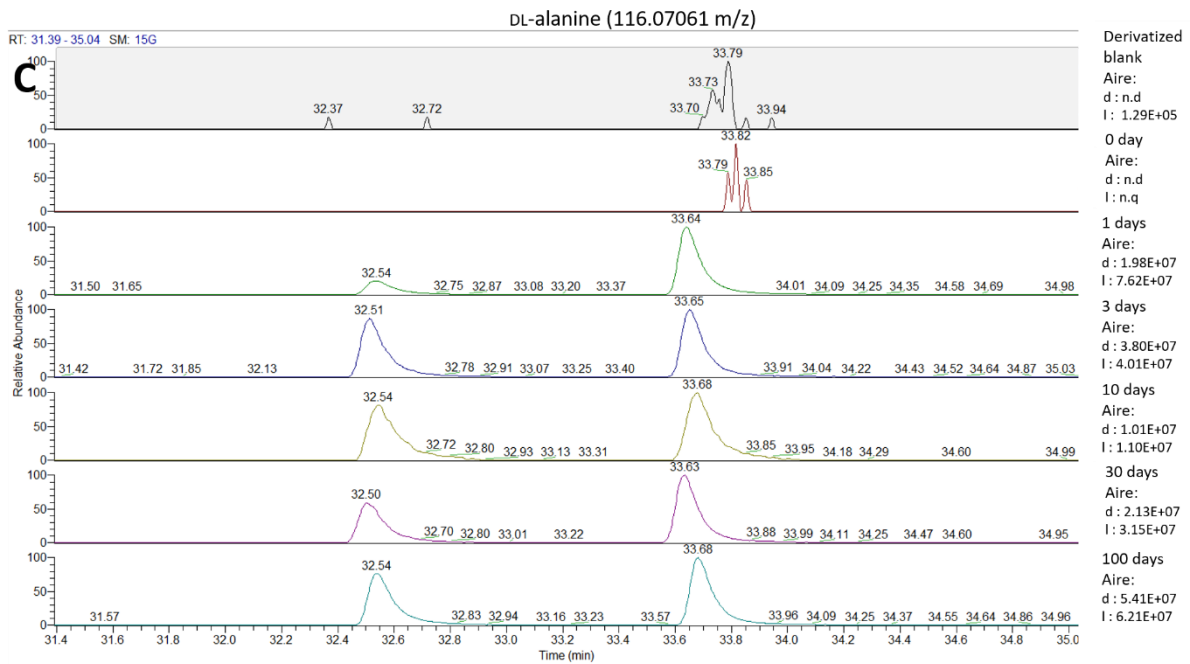
508



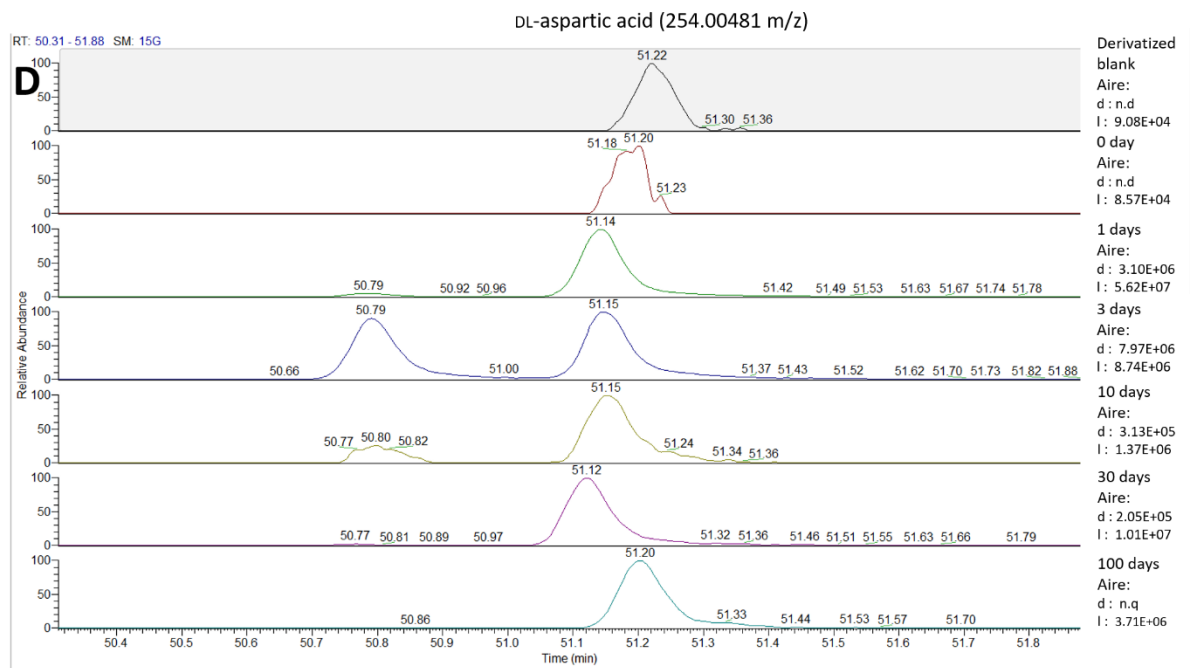
509



510



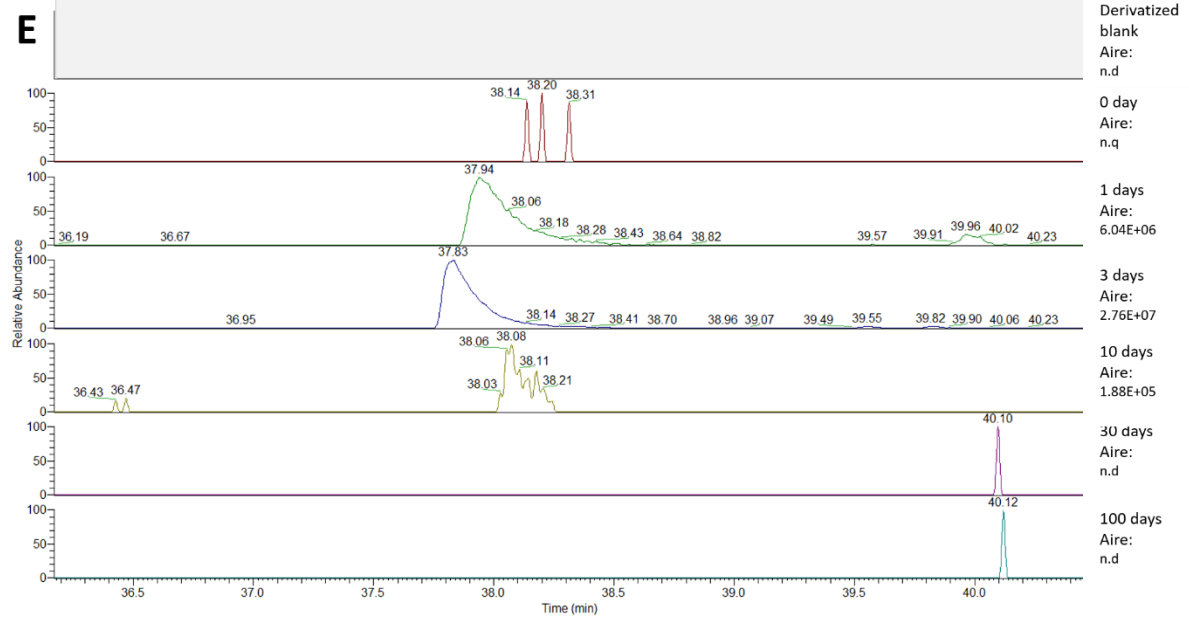
511



512

β -alanine (270.03579 m/z)

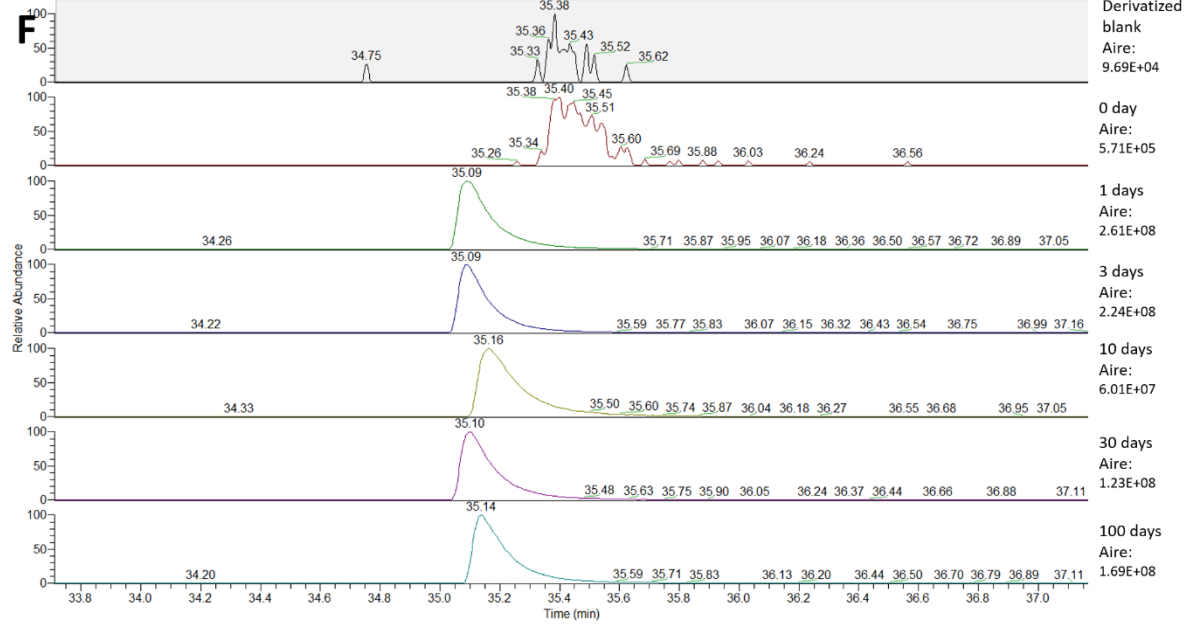
RT: 36.17 - 40.46 SM: 15G



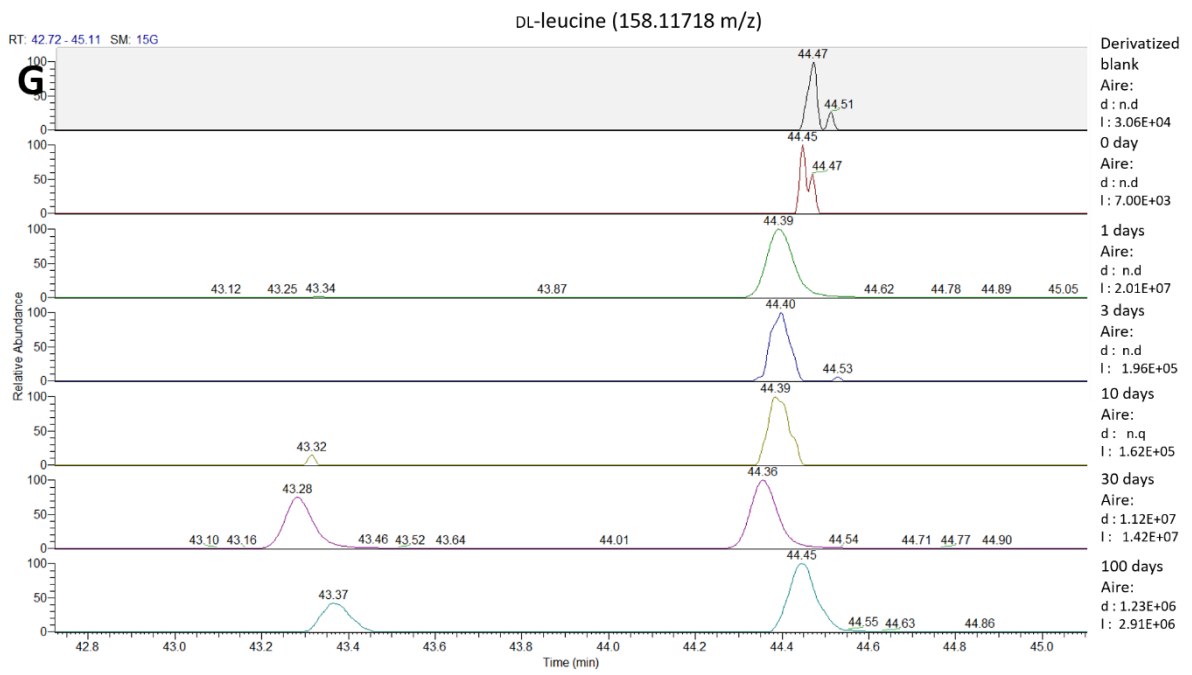
513

glycine (102.05496 m/z)

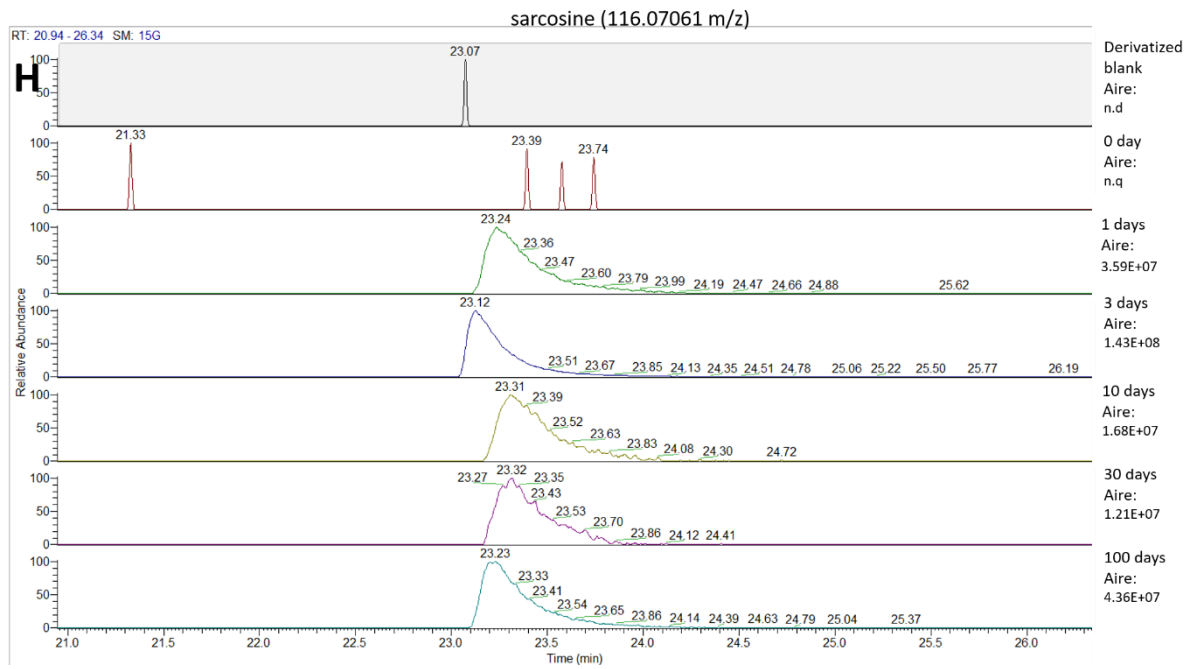
RT: 33.71 - 37.17 SM: 15G



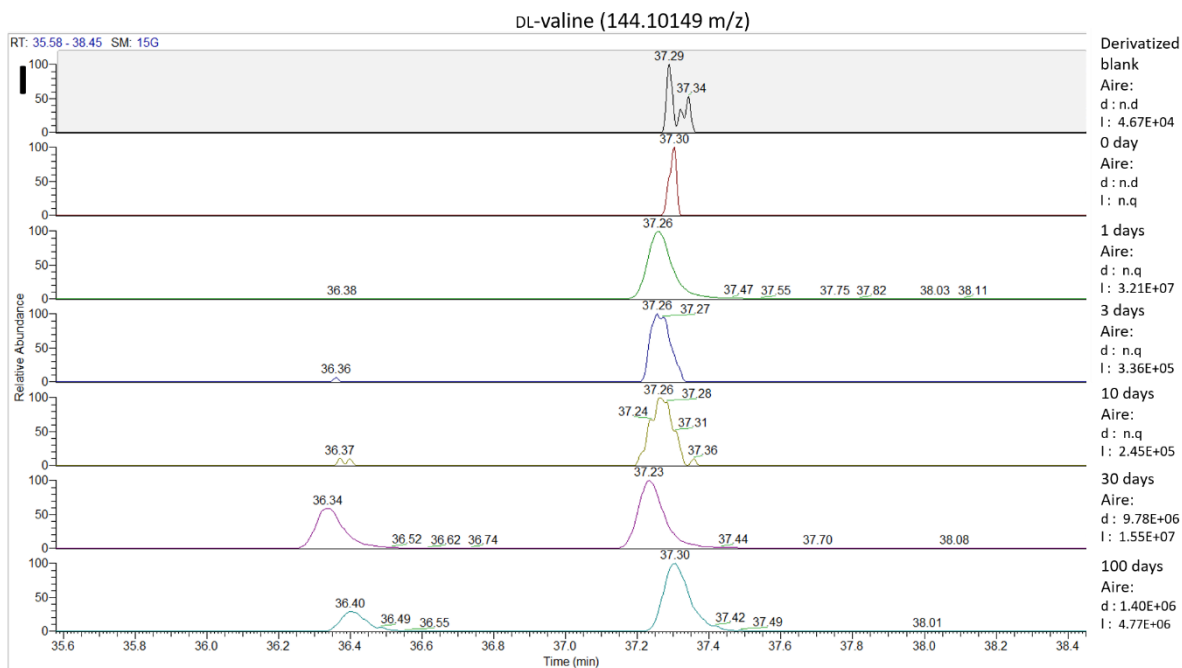
514



515



516



517

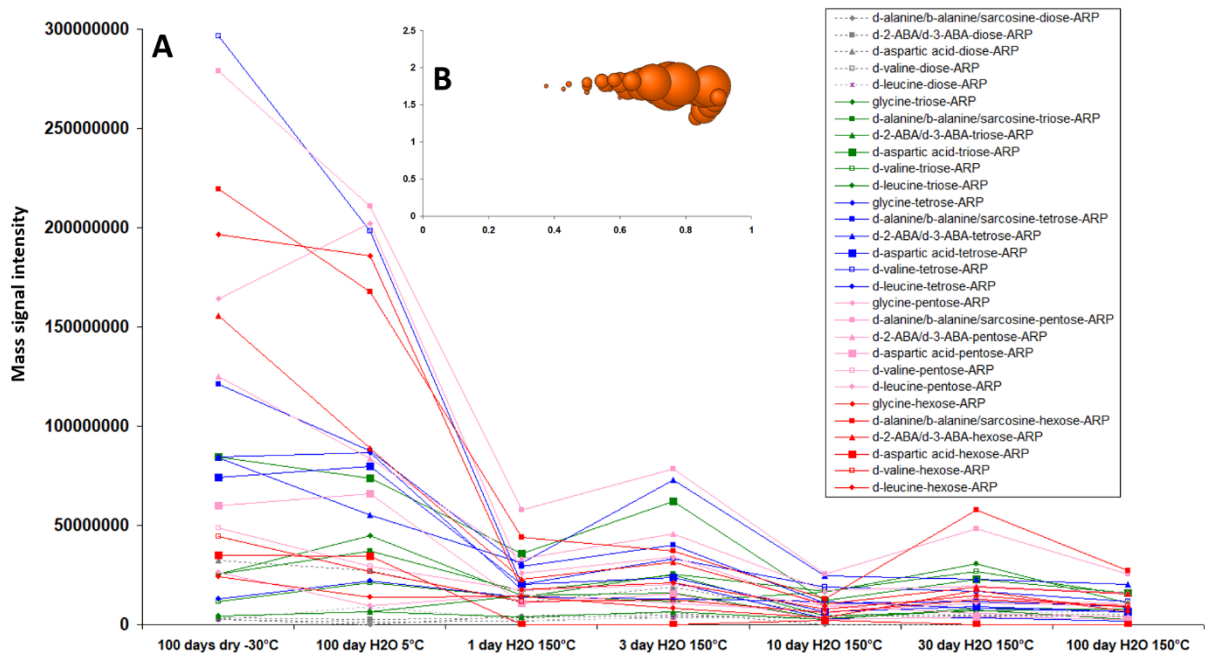
518 **Figure S4 - Chromatograms of the different amino acids monitored during the aqueous alteration of pre-**
 519 **accretional organic analog at 150 °C under 6 bars for different duration (0 day corresponds to the initial**
 520 **pre-accretional analog, 1, 3, 10, 30 and 100 days). All data are mass extraction of the characteristic mass**
 521 **of a given amino acids on full scan. Are also reported the derivatized blank with the extracted mass**
 522 **corresponding to the one of the amino acid monitored. n.d: not detected, n.q: detected but under the limit**
 523 **of quantification. (A) DL-2-ABA, (B) DL-3-ABA, (C) DL-alanine, (D) DL-aspartic acid, (E) β -alanine, (F)**
 524 **glycine, (G) DL-leucine, (H) sarcosine, and (I) DL-valine.**

525

Theoretical m/z	Exp. m/z	Neutral formula	Amadori rearrangement product (ARP)	100 days dry -30°C	100 day H2O 5°C	1 day H2O 150°C	3 day H2O 150°C	10 day H2O 150°C	30 day H2O 150°C	100 day H2O 150°C
130.05096	130.05097	C5H9NO3	alanine/b-alanine/sarcosine-glycolaldehyde-ARP	2504102	0	4210929	5894227	0	0	0
144.06661	144.06662	C6H11NO3	2-ABA/d-3-ABA-glycolaldehyde-ARP	3396545	2646139	3261884	4609152	3116913	3452400	2945875
174.0407	174.04079	C6H9NO5	aspartic acid-glycolaldehyde-ARP	32279092	26941404	11379647	19023838	4660976	4160652	4279944
158.08226	158.08225	C7H13NO3	valine-glycolaldehyde-ARP	2797453	1447346	1697093	3666564	4045417	4751750	5021589
172.09791	172.09793	C8H15NO3	leucine-glycolaldehyde-ARP	2464198	8994665	2327955	3279901	3999619	5680488	6898776
146.04588	146.04588	C5H9NO4	glycine-triose-ARP	25319092	44844088	14673530	16048065	2969381	7242917	2404041
160.06153	160.06153	C6H11NO4	alanine/b-alanine/sarcosine-triose-ARP	25382206	37197804	16770200	25017896	4485142	6724031	7736155
174.07718	174.07685	C7H13NO4	2-ABA/d-3-ABA-triose-ARP	4145765	6250220	3895090	6620017	2780961	8048164	7625521
204.05136	204.05135	C7H11NO6	aspartic acid-triose-ARP	84323056	73907280	35776120	62137104	12129185	22705778	15843103
188.09283	188.09283	C8H15NO4	valine-triose-ARP	11484519	21144504	13934038	25349746	17008968	26520988	15194823
202.10848	202.10848	C9H17NO4	leucine-triose-ARP	4211419	6438216	14764764	11566977	16264553	30503730	10765309
176.05644	176.05645	C6H11NO5	glycine-tetrose-ARP	84315360	86590232	17822524	21160816	3067418	3402872	1856640
190.07209	190.07210	C7H13NO5	alanine/b-alanine/sarcosine-tetrose-ARP	121093376	87451672	29142686	40090436	10930415	11505112	9230080
204.08774	204.08775	C8H15NO5	2-ABA/d-3-ABA-tetrose-ARP	84142872	55192704	31110832	72696648	24399826	22824616	20070228
234.06192	234.06192	C8H13NO7	aspartic acid-tetrose-ARP	73953000	79589704	20054210	23658860	6643664	9128619	6440824
218.10339	218.10339	C9H17NO5	valine-tetrose-ARP	29660786	198238048	20410032	33061466	19158206	16651592	11732101
232.11904	232.11903	C10H19NO5	leucine-tetrose-ARP	12757804	22031454	13796020	12930018	11783099	8200392	6276579

206.06701	206.06701	C7H13NO6	glycine-pentose-ARP	164205824	202090336	25909804	33922740	9358810	5615057	3679322
220.08266	220.08265	C8H15NO6	alanine/b-alanine/sarcosine-pentose-ARP	278809824	210757344	57972504	78336640	25412460	48362912	25371796
234.09831	234.09831	C9H17NO6	2-ABA/d-3-ABA-pentose-ARP	124923640	83759456	33237214	45490564	17321954	19191494	16100242
264.07249	264.07251	C9H15NO8	aspartic acid-pentose-ARP	59848004	65914880	10756142	15339759	2558129	3997815	2379849
248.11396	248.11394	C10H19NO6	valine-pentose-ARP	48825248	29257260	17254268	20095680	9543400	12939840	10325266
262.12961	262.12957	C11H21NO6	leucine-pentose-ARP	26321682	9651431	14873353	10743133	6626378	10743073	9498359
236.07757	236.07757	C8H15NO7	glycine-hexose-ARP	196473472	185832976	17743568	21104354	7854022	14654591	8492283
250.09322	250.09321	C9H17NO7	alanine/b-alanine/sarcosine-hexose-ARP	219514352	167719312	44102784	37062336	12943750	57663092	27158798
264.10887	264.10887	C10H19NO7	2-ABA/d-3-ABA-hexose-ARP	155620688	88672272	23005254	31547648	10418876	19150982	15342169
294.08305	294.08299	C10H17NO9	aspartic acid-hexose-ARP	34784644	34406720	0	0	2069278	0	0
278.12452	278.12453	C11H21NO7	valine-hexose-ARP	44238992	26914982	11805090	12690546	5969606	12416931	9540219
292.14017	292.14016	C12H23NO7	leucine-hexose-ARP	24265132	13956379	14375043	8201023	3550577	17184396	6656929

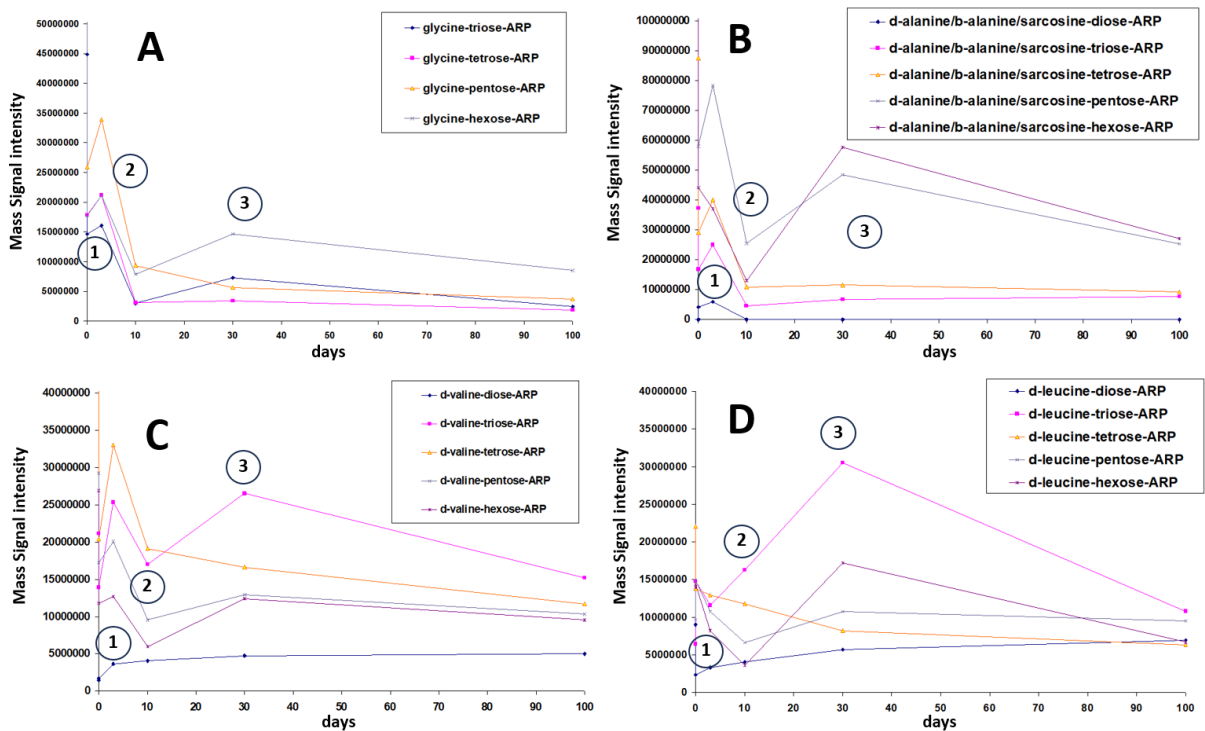
526 **Table S1 - All possible Amadori rearrangement products (ARP) as obtained in reaction of the measured amino acids with glycolaldehyde and possible reducing**
527 **sugars, including triose, tetrose, pentose, and hexose. Corresponding ARP with its neutral formula, theoretical and experimental mass of the deprotonated ions, as**
528 **well as the intensity of these ions in the original material and the hydrothermal kinetic at 150°C during the 100 days.**



529

530 Figure S5 - (A) Time evolution of the various ARPs during hydrothermal process; (B) position in the van
 531 Krevelen diagram of the considered ARPs.

532



533

534 Figure S6 - (A)-(D) Time evolution of the individual ARPs (to be compared to the evolution of the
 535 individual amino acids in Figure 2) during the hydrothermal process